Title
LOW-PRESSURE HYDROGEN/OXYGEN FLAME STUDIES

Permalink
https://escholarship.org/uc/item/22t0x51n

Author
Brown, N.J.

Publication Date
1978-06-01

Lawrence Berkeley Laboratory
UNIVERSITY OF CALIFORNIA

ENERGY & ENVIRONMENT DIVISION

LOW-PRESSURE HYDROGEN/OXYGEN FLAME STUDIES

N. J. Brown, K. H. Eberius, R. M. Fristrom,
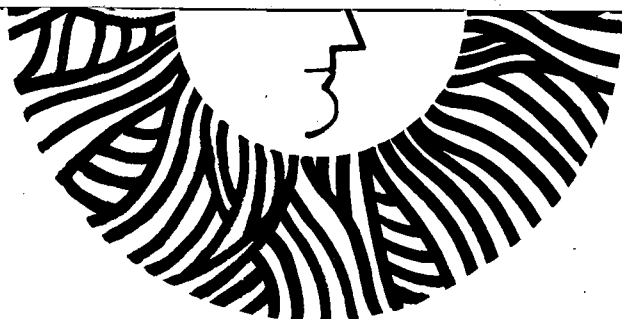K. H. Hoyermann and H. Gg. Wagner

June 1978

DISCLAIMER

Low-Pressure Hydrogen/Oxygen Flame Studies

N. J. BROWN*

Department of Mechanical Engineering, University of California, Berkeley, California 94720

K. H. EBERIUS

DFVLR, Institut für Reaktionskinetik, 7000 Stuttgart 80, West Germany

R. M. FRISTROM*

Johns Hopkins University, Applied Physics Laboratory, Laurel, Maryland 20810

K. H. HOYERMANN and H. Gg. WAGNER

Institut für Physikalische Chemie der Universität Göttingen, West Germany

Composition and temperature profiles are reported for lean, near stoichiometric and rich, low-pressure hydrogen/oxygen flames. A discussion of the consistency checks used to assure the soundness of the analysis and various methods to estimate radical concentrations is presented. The mechanism of water formation in the various flame systems is discussed.

I. INTRODUCTION

Although studies of premixed laminar flames have contributed much toward the understanding of combustion, many of the mechanistic details of specific flame chemistries still remain elusive. There are two major reasons for this. First, interpretation of flame structure depends upon a proper description of transport phenomena. This requires values of several transport coefficients as a function of temperature and mixture composition, and these values are presently obtained from model calculations. In addition, transport analysis requires composition and temperature gradients which are often steep and difficult to evaluate. Second, most of the important flame reactions involve free radical species which are extremely difficult to quan-

tify since they are highly reactive and thus occur in relatively low concentrations.

This paper reports on experimental studies of lean, near stoichiometric and rich hydrogen/oxygen flames. Hydrogen/oxygen flames have been studied previously by many investigators [1-3] and more recently by Eberius et al. [4] and Dixon-Lewis and collaborators [5]. Moreover, this flame system, whose chemistry plays an important role in all hydrocarbon combustion, still warrants additional study to further clarify the chemistry and to provide data for comparison with modeling studies.

The paper has the following organization. Section II of the paper provides a description of the experimental techniques used to measure temperature and species profiles. The results are presented in Section III. Flame profiles are given, and the consistency checks employed to ascertain the soundness of the structure analyses, and the associated data are discussed. Radical species measurements and techniques to estimate radical concen-

TABLE I

Initial Composition, Pressure, and Velocity of the
Hydrogen–Oxygen Flame Studied

Flame	H_2	O_2	N_2	P(torr)	v_0(cm/sec)
I	15	85	–	14.6	26.4
IIa	48	52	–	7.2	223
IIb	27	28	45	7.2	159
III[a]	81	19	–	7.7	156

All compositions are given in mole percent.
[a] previously reported.

trations are then presented. Finally, the section is
concluded with a discussion of the mechanisms for
water formation in hydrogen/oxygen flames of dif-
ferent equivalence ratios.

II. EXPERIMENTAL MEASUREMENTS

Initial compositions, pressures, and velocities of
the flames are given in Table 1, which includes data
associated with a previously reported [4] rich
flame for comparison and completeness. A brief
discussion of the techniques used to determine
composition and temperature profiles is given in
subsequent paragraphs.

The flames were stabilized on water-cooled
sintered bronze plates ranging from 5 to 40 cm
across. Temperatures were measured with 0.1 mm
diameter silica coated Pt/Pt-Rh thermocouples.
Radiation losses were compensated by electrical
heating for a few cases to determine emissivity
which was then used to correct the remaining
thermocouple measurements. Temperature was
also determined by measuring the relative absorp-
tion of OH rotational transitions.

Gas samples were withdrawn from the flame
with quartz microprobes having orifice diameters
ranging from 50 to 100 μm. Concentrations of the
stable species, H_2, N_2, O_2, and H_2O were meas-
ured with gas chromatography and mass spectrom-
etry to a relative precision of less than 1.0 percent.
An attempt to measure H and O concentrations
quantitatively with microprobing and ESR detec-
tion was unsatisfactory in all but the rich flame. In
the rich flame, H atoms could be measured since
OH and O radical concentrations were low enough

to reduce the homogeneous reactions which occur
in the probe. The precision of this measurement
ranged between 3 and 5%.

Concentration profiles of OH were determined
with ultraviolet absorption spectroscopy through
investigation of the (0, 0) band of the $^2\Sigma$-$^2\pi$ sys-
tem assuming only weak absorption and Doppler
line broadening. The oscillator strength used was
8.0 × 10^{-4} which compares favorably with that
of Lerner [6]. The OH rotational levels were char-
acteristic of an equilibrium distribution, thus pro-
viding an indication of sufficient spectroscopic
resolution and one-dimensional behavior. The rela-
tive precision of various OH measurements ranged
from 3 to 5%.

Infrared spectroscopic searches were made for
HO_2 and H_2O_2 in the wavelength region 1 to 15
microns on a rectangular 40 × 10 cm burner using
a multiple reflecting system of the White-Herzberg
type which gave approximately 60 traversals
through the flame. HO_2 was below the limit of
detectability. If one uses the estimated absorption
coefficient of Hunziker and Wendt [7], the limit
of detectability corresponds to an HO_2 concen-
tration of 0.01 mole percent. H_2O_2 was, however,
detected in the rich flame, III, where absorption
measurements indicated concentrations below 0.1
mole percent and emission measurements indi-
cated approximately 0.02 mole percent.

III. RESULTS AND CONCLUSIONS

A. Concentration and Flux Profiles

Flame structure analysis consists of using physical
laws and transport coefficients to convert indi-
vidual species concentration profiles to flux pro-
files which are, in turn, differentiated to determine
the net reaction rate of that species. One of the
important uses of the net rate data is the determin-
ation of mechanistic information. A mechanism is
postulated, and the net rate data are then used to
determine rate coefficients of specific reactions.
These are, in turn, checked against literature values
to ascertain the viability of the mechanisms.

Figures 1, 2, and 3 show the smoothed compo-
sition and temperature profiles for flames I, IIa,
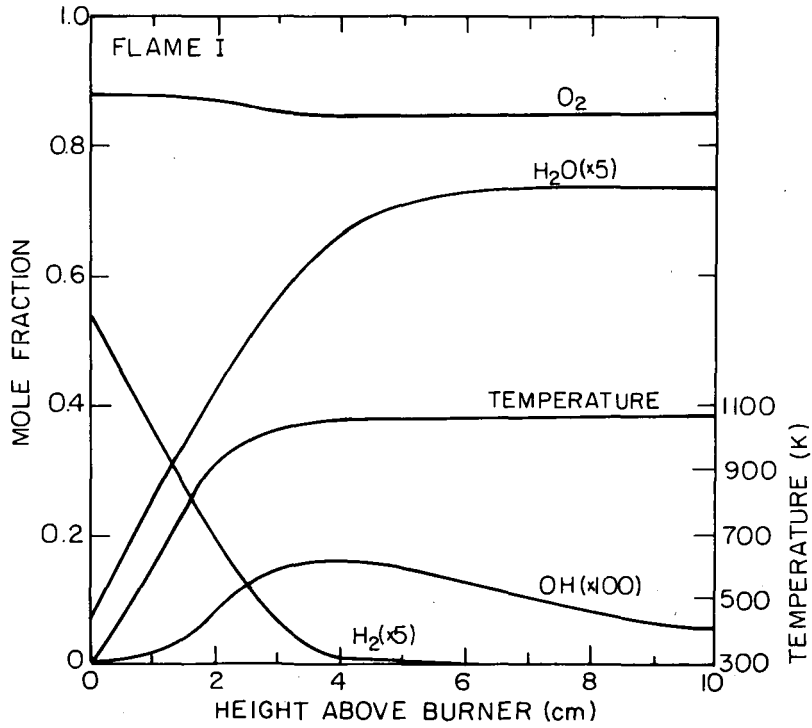and IIb, respectively. Data points were taken at

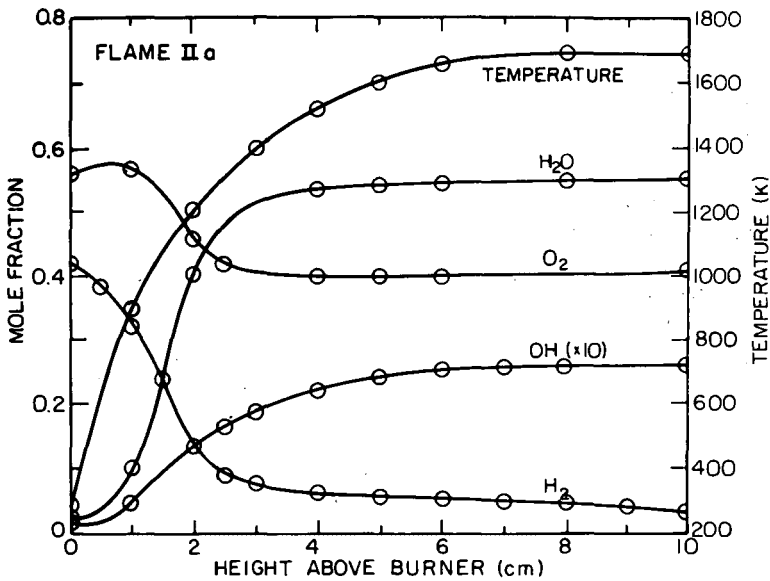Fig. 1. Temperature (K) and composition (mole fraction) profile for Flame I.

Fig. 2. Temperature (K) and composition (mole fraction) profile for Flame IIa.
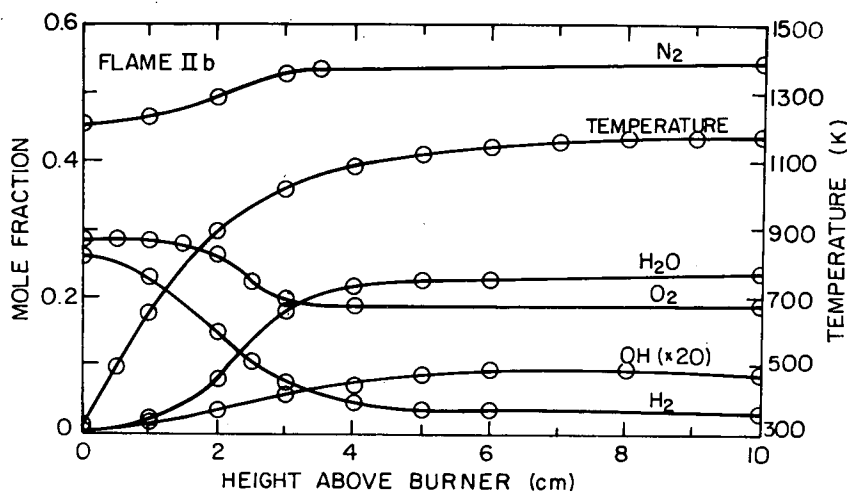
Fig. 3. Temperature (K) and composition (mole fraction) profile for Flame IIb.

0.5 mm intervals, and smooth curves were drawn through the points. The points on the profiles in Figs. 2 and 3 are experimental values. Although experimental data were taken every 0.5 mm, only data points of the approximate density of every 0.5 cm are shown. The plotted points are typical, and most of the points of the complete data set fell on the smoothed curves. Note the simple, single-stage nature of hydrogen combustion, which characterizes it from two-stage hydrocarbon combustion. Flame I, which represents the leanest flame that could be stabilized on the 19 cm burner (inflection point of the temperature profile at the burner surface), had a maximum temperature of 1080 K and a maximum OH concentration of 0.16 mole percent. Flames IIa and IIb are interesting to compare since they have nearly equal initial H_2/O_2 ratios and differ by nitrogen dilution. After the effect of dilution is accounted for (through normalization), both the OH and H_2O concentrations are greater in the undiluted flame, IIa.

Flux, n_i, is computed from concentration using the relationship

$$n_i = N_i(v + V_i) \qquad (1)$$

where v is the mass velocity, and N_i and V_i are respectively the molar concentration and diffusion velocity of species, i. Diffusion velocities were computed using the binary mixture approximation

for Flames I and II and the multicomponent mixture approximation [8] for Flame III. The binary diffusion coefficients were computed using a Lennard-Jones (12-6) potential, with the potential parameters and temperature dependence taken from standard texts [8, 9]. The required derivatives of the concentration profiles were determined graphically, and the derivative curves were smoothed. Figure 4 shows the mole flux profiles for the stable species of Flame IIa. An interesting
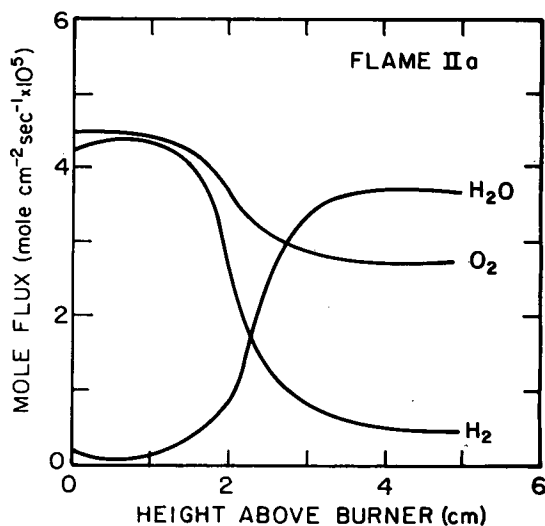

Fig. 4. Mole flux (mole·cm^{-2}·sec^{-1} × 10^5) profile for stable species for Flame IIa.

point regarding the interaction of flow and transport in flames is illustrated through comparison of the composition and mole flux profiles of Flame IIa. In the main reaction zone, H_2 is seen to move at a velocity twice the center of mass, whereas H_2O is slower, moving at approximately one-half the center of mass velocity.

B. Consistency Checks

Since composition and temperature measurements are made only at a finite number of points in the flame, and the precision is limited experimentally, some consistency checks should be made on the data and data reduction procedures to establish that they are of adequate quality to extract information about the flame chemistry. Graphs associated with Flame IIa are used in the following to illustrate the various checks made to establish consistency.

When determining flux and rate parameters, the derivatives of the composition profiles are calculated from the experimentally measured values. One check for consistency comes from the relationship between various mole fractions, X_i

$$\sum X_i = 1 \tag{2a}$$

which yields a test for the derivatives

$$\sum \frac{d}{dz}(X_i) = 0. \tag{2b}$$

Even though the flames considered had regions of steep gradients, the following inequality:

$$\sum \frac{d}{dz}(X_i) < 10^{-4} \text{ cm}^{-1}$$

was obtained for all positions in the flames. Typical maximum concentration gradients are approximately 0.2 cm^{-1}, so that having the sum (2b) cancel to 10^{-4} cm^{-1} along the profile reflects a sound analysis.

A second check is that in the center of mass, the relative value of the weighted sum of the dif-
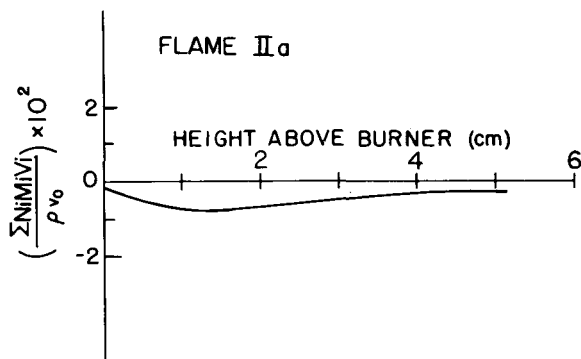

Fig. 5. Relative weighted sum of diffusion velocities profile for Flame IIa.

fusion velocities must be zero by definition, that is

$$\frac{\sum_i N_i M_i V_i}{\rho^0 v^0} = 0 \tag{3}$$

where M_i is the molecular weight of the ith species. Figure 5 is a profile of this function, $\Sigma_i N_i M_i V_i / \rho^0 v^0$, for Flame IIa. The superscript 0 denotes initial values in the cold gas. In this and the other flames considered, the absolute value of (3) is less than one percent. Since this test involves concentrations, their derivatives, and associated transport coefficients which are temperature dependent, a relative error of less than one percent provides an additional indication that the analysis is sound.

A third check is the pointwise conservation of individual elemental fluxes which is expressed mathematically as:

$$\frac{d}{dz}\left(\sum_i v_{ij} G_i / M_i\right) = 0 \tag{4}$$

where v_{ij} is the number of atoms j in the ith chemical species and G_i is the ith species mass flux fraction. An example of elemental flux profiles for hydrogen and oxygen where the sum has included only stable species is shown for Flame IIa in Fig. 6. Deviations from the initial value are less than 8 percent for all flames considered. These deviations result from misalignments of temperature and composition profiles, errors in experimental measurements and transport coefficients, and the omission of radical species contributions.
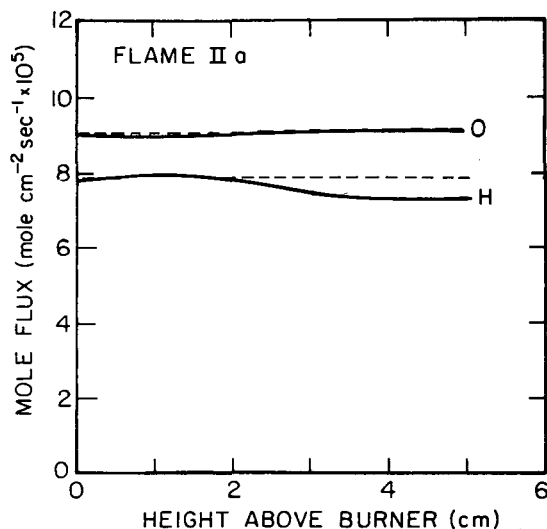
Fig. 6. Elemental mole flux (mole·cm^{-2}·sec^{-1} × 10^{-5}) profile for Flame IIa. Dashed lines indicate initial values.

C. Estimation of Radical Concentrations

Attempts to measure H and O atoms by probing and ESR were not successful in some flames due to the complications introduced by heterogeneous recombination reactions and the low activation energy homogeneous reactions

$$O + OH \rightarrow O_2 + H$$

$$OH + OH \rightarrow H_2O + O$$
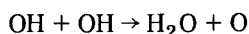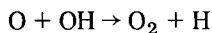
which can occur in sampling probes. Probe lengths were varied to determine the effect of probe reactions on radical concentration measurements. The logarithm of the concentration of H and O atoms decayed linearly with increasing probe length. If the homogeneous reactions are dominant, an increase in H atom concentrations would be observed. Hence it is assumed that extrapolation to zero probe length accounts for the wall reactions. It was concluded that ESR measurements of O and H radicals are only satisfactory in those experiments in which the homogeneous reactions are relatively unimportant, so that one can use extrapolation to account for the wall reactions. This condition obtains when the H or O concentration dominates the radical pool. This situation was

realized in the previously reported Flame III where H atom concentrations were measured with ESR since the H atom concentrations were considerably larger than O and OH. In Flame IIa, where the radical concentrations are comparable (the worst possible case), H and O concentrations are estimated, through ESR measurement, to be 4 to 5 percent in the main reaction zone.

The use of energy conservation to determine radical concentrations was also attempted since radical species are large carriers of enthalpy and make important contributions to the energy balance in a flame. This method proved unsuccessful due to uncertainties in transport coefficients as a function of composition and temperature and misalignment of species and temperature profiles.

A third method which is often invoked to determine radical concentrations is the use of the partial equilibrium hypothesis. This method was first proposed by Bulewicz et al. [1] and was successfully applied to the hot gas zone of $H_2/O_2/N_2$ flames. Certain fast bimolecular reactions become balanced such that the associated mass action expression is equal to the equilibrium constant at temperatures prior to the thermodynamic equilibrium temperature. In a state of partial equilibrium, the absolute concentrations are different from those at true equilibrium.

The kinetic data associated with the hydrogen/oxygen system are given in Table II and are taken from Baulch et al. [10] with the exception of rate data [11] associated with molecular oxygen dissociation. The equilibrium constants for the bimolecular reactions K_i are the fitted values given in Kondratiev [12]. The partial equilibrium assumed here involves the fast shuffling bimolecular reactions of Table 2, (b1) through (b3) and the associated equilibrium constants K_1, K_2, and K_3. These equilibrium expressions yield three equations which can be solved for three concentrations, provided that three concentrations have been measured. Here, the concentrations of four species, H_2, O_2, OH, and H_2O have been measured so that one species can be computed two ways and agreement can provide an indication of the validity of the partial equilibrium hypothesis. The equilibrium expression associated with reaction (b3) was solved

TABLE 2
Kinetic Mechanism of the Hydrogen/Oxygen System

Hydrogen-Oxygen Reactions				
Bimolecular[a]	A_f	$E_f{}^c$	A_r	$E_r{}^c$
b1. H + O$_2$ $\rightleftharpoons$ OH + O	2.2×10^{14}	16,800	1.3×10^{13}	0
b2. O + H$_2$ $\rightleftharpoons$ OH + H	$1.8 \times 10^{10}T$	$8900 + 1.987T$	$8.3 \times 10^9 T$	$6950 + 1.987T$
b3. OH + H$_2$ $\rightleftharpoons$ H$_2$O + H	2.2×10^{13}	5150	9.3×10^{13}	20,360
b4. OH + OH $\rightleftharpoons$ H$_2$O + O	6.3×10^{12}	1100	6.8×10^{13}	18,350
b5. HO$_2$ + H $\rightleftharpoons$ 2OH	2.5×10^{14}	1900	1.2×10^{13}	40,100
b6. HO$_2$ + (H, O, OH) $\rightleftharpoons$ O$_2$ + (H$_2$, OH, H$_2$O)				
Termolecular[b]				
t1. H + H + M $\rightleftharpoons$ H$_2$ + M	$6.4 \times 10^{17}T^{-1}$	–	2.2×10^{14}	96,000
M = Ar				
t2. O + O + M $\rightleftharpoons$ + M			$2.6 \times 10^{18}T^{-1}$	118,700
M = Ar				
t3. H + OH + M $\rightleftharpoons$ H$_2$O + M	$2.2 \times 10^{22}T^{-2}$	–	1.3×10^{15}	105,000
M = N$_2$				
t4. H + O$_2$ + M $\rightleftharpoons$ HO$_2$ + M	1.6×10^{15}	–1000	2.1×10^{15}	45,900
M = Ar				

[a] units of bimolecular A cm^3 mole^{-1} sec^{-1}.

[b] units of termolecular A cm^6 mole^{-2} sec^{-1}.

[c] units of E$_f$ and E$_r$, cal/mole.

for hydrogen atom concentration:

$$(\text{H}) = \frac{K_3(\text{H}_2)(\text{OH})}{(\text{H}_2\text{O})} \qquad (5)$$

and this expression for (H) was then substituted into the equilibrium expressions associated with reactions (1) and (2) to obtain two equations for oxygen atom concentration:

$$(\text{O}) = \frac{K_1 K_3(\text{H}_2)(\text{O}_2)}{(\text{H}_2\text{O})} \qquad (6)$$

$$(\text{O}) = \frac{K_3}{K_2} \frac{(\text{OH})^2}{(\text{H}_2\text{O})} \qquad (7)$$

Making the identification $K_3/K_2 = K_4$, Eq. (7) is identical to that derived assuming partial equilibration of reaction (b4).

Figure 7 shows the measured hydroxyl concentrations and estimated (via partial equilibrium) hydrogen and oxygen atom concentrations for Flame I. The two oxygen atom concentrations calculated via partial equilibrium agree within a factor
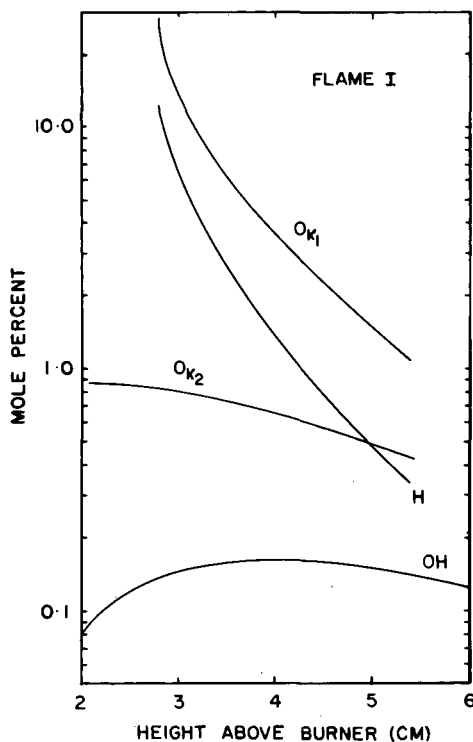

Fig. 7. Radical concentrations (mole percent) for Flame I. O$_{K_1}$ calculated via Eq. (6); O$_{K_2}$ calculated via Eq. (7), H calculated via Eq. (5); and OH measured spectroscopically.
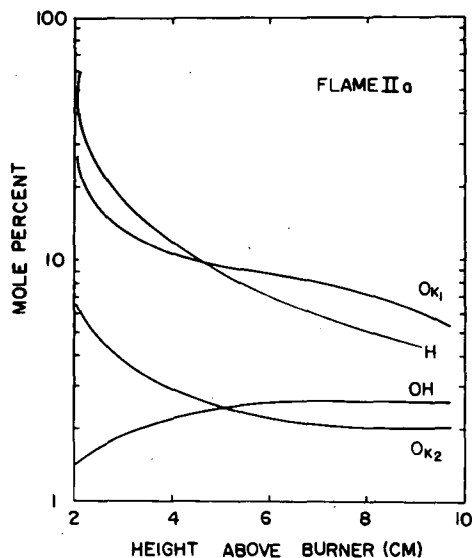
Fig. 8. Radical concentrations (mole percent) for Flame II. O_{K_1} calculated via Eq. (6); O_{K_2} calculated via Eq. (7); H calculated via Eq. (5); and OH measured spectroscopically.

of 3 beyond a distance of 5.0 cm height above burner, at the beginning of the post-flame zone where flame temperatures are approximately 1070 K. Figure 8 is the analogous plot for Flame IIa which shows the agreement between the two partial equilibrium values for the oxygen atom varies between a factor of 4 and 2.7, between 6 and 10 cm height above burner, respectively, well into the post-flame zone. The agreement for Flame III is less satisfactory, and is only less than a factor of 4 well into the post-flame zone, at distances greater than 7 cm.

Assuming reliable primary data, these results illustrate that reactions (b1) through (b4) are not simultaneously balanced in the primary reaction zone and that partial equilibrium approximations are only appropriate for estimating radical concentrations in the post-flame zone. Moreover, the application of the partial equilibrium approximation in the manner described is not suitable for determining which of the bimolecular reactions is balanced. Furthermore, there is some evidence that (b4) is equilibrated first. First, oxygen atom concentrations calculated via Eq. (7) are more in line with values that one might expect for radical concentrations. Second, mass conservation for oxygen, including stable oxygen containing species and hydroxyl radical, was also used to estimate oxygen atom concentrations for Flame III, and the values determined agreed more closely with values computed via Eq. (7). Biordi et al. [13] also found reaction (b4) which is associated with Eq. (7) to be equilibrated early in low-pressure stoichiometric methane flames.

D. Mechanism of Water Formation

Several mechanisms for the formation of water are possible in hydrogen/oxygen flames of different equivalence ratios. One of these involves the bimolecular reactions (b3) and (b4). One would expect this mechanism to be important in the high-temperature portion of low-pressure flames which take long distances (times) to reach thermodynamic equilibrium. Another mechanism often proposed involves the HO_2 radical and both the bimolecular step (b6) and termolecular steps (t3) and (t4). One might expect this mechanism to be important at low temperatures and high H atom concentrations.

Here, water production in the high-temperature (greater than 700 K) portion of the flame was investigated. It was first assumed that reaction (b3) was the principal source of water. The rate coefficient as a function of temperature was determined as:

$$k_{OH+H_2} = \frac{1}{(OH)(H_2)} \frac{d}{dz} [N_{H_2O}(v + V_{H_2O})]$$

for different points along the profile for Flames I, IIa as shown in Fig. 9. Data from the previously reported Flame III are also shown. The points for Flames IIa and III correspond to 1 mm distances in the flame, while only representative points are shown for Flame I. The suggested Arrhenius line [10] is drawn for comparison. The rate coefficient derived from the data (determined neglecting the low-temperature point for Flame I) is:

$$k_{H_2+OH} = 1.2 \times 10^{13} \exp(-5300/RT) \frac{cm^3}{mole/sec}$$

which is in reasonable agreement with the value

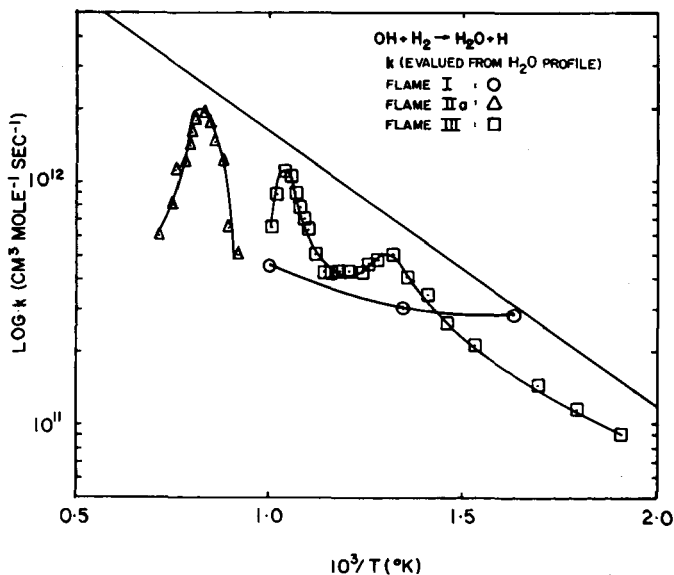Fig. 9. Log k(cm³·mole⁻¹·sec⁻¹) for $OH + H_2 \rightarrow H_2O + H$ as a function of $10^3/T(K)$ determined from flame data. Line indicates suggested value from reference 10.

given in Table 2. This reaction appears to be the principal source of water production at temperatures above 700 K to temperature prior to the onset of partial equilibrium. The value also agrees quite well with the results of the earlier study [4]. We estimate that eighty percent of the water formation for these flame systems is due to reaction (b3) and that the decay in the rate coefficient in the high-temperature region of the individual flames reflects the neglect of the reverse of reaction (b3). The effect of the reverse reaction (b3) can only be assessed for Flame III where H atom concentrations are determined via probing and ESR. The reverse rate is 0.1 at 500 K and 5% at 1000 K of the forward rate. One can estimate the ratio of rates for Flames I and IIa using partial equilibrium approximations for H atom which overestimate H atom and thus the reverse rate. The reverse rate was less than 6% for various points on the profile for both flames. The termolecular recombination (t3) contributes less than one percent of the total water production in the main reaction zone. Reaction (b4) was considered as a possible step in the water formation mechanism for Flames I and II; however, it accounted for less than 2 percent in II and less than 20 percent in I.

REFERENCES

1. Bulewicz, E. M., James, C. G., and Sugden, T. M., Photometric Investigation of Alkali Metals in Hydrogen Atoms in Burnt Gas Mixtures, *Proc. R. Soc., London* A235, 89, (1956).

2. Kaskan, W. E., Hydroxyl Concentrations in Rich Hydrogen/Air Flames Held on Porous Burners, *Combust. Flame* 2, 229 (1958).

3. Dixon-Lewis, G., Flame Structure and Flame Reaction Kinetics. I. Solution of Conservation Equations and Application to Rich Hydrogen-Oxygen Flames, *Proc. R. Soc., London* A298, 495 (1966).

4. Eberius, K. H., Hoyerman, K., and Wagner, H. Gg., Experimental and Mathematical Study of a Hydrogen/Oxygen Flame, *Thirteenth Symposium (International) on Combustion*, The Combustion Institute, Pittsburg, p. 713.

5. Dixon-Lewis, G., Flame Structure and Flame Reaction Kinetics. VII. Reactions of Traces of Heavy Water, Deuterium and Carbon Dioxide Added to Rich Hydrogen + Nitrogen + Oxygen Flames, *Proc. R. Soc., London* A330, 219 (1972), and VIII, *ibid* A331, 571 (1973).

6. Lerner, R. C. M., The Influence of Vibration-Rotation Interaction on Intensities in the Electronic Spectra of Diatomic Molecules, *Proc. Roy. Soc., London* A269 311 (1962).

7. Hunziker, H. E., and Wendt, H. R., *J. Chem. Phys.* 60, 4622 (1974).

8. Fristrom, R. M., and Westenberg, A. A., *Flame Structure*, McGraw-Hill, New York, 1965.

9. Hirschfelder, J. O., Curtiss, C. F., and Bird, W. B., *Molecular Theory of Gases and Liquids,* John Wiley and Sons, Inc., New York, 1967.

10. Baulch, D. L., Drysdale, D. D., Horne, D. G., and Lloyd, A. C., *Evaluated Kinetic Data for High Temperature Reactions,* Butterworths, London, (1972) Vol. I.

11. Johnston, H. S., Gas Phase Reaction Kinetics of Neutral Oxygen Species, NBS-NSRDS-20, 1968. (Supt. of Documents, U.S. Govt. Printing Office, Washington, D.C. 20402).

12. Kondratiev, V. N., *Rate Constants of Gas Phase Reactions, Reference Book,* R. M. Fristrom, Ed. Translated by L. J. Holtschlag, COM-72-10014, Office of Standard Reference Data, NBS, 1972.

13. Biordi, J. C., Lazzara, C. P., and Papp, J. F., An Examination of the Partial Equilibrium Hypothesis and Radical Recombination in 1/20 atm Methane Flames, *Sixteenth Symposium (International) on Combustion,* The Combustion Institute, Pittsburgh, p. 1097.